Repositorio Institucional de la Universidad Autónoma de Madrid

https://repositorio.uam.es

Esta es la **versión de autor** del artículo publicado en:
This is an **author produced version** of a paper published in:

ACS Photonics 5.1 (2018): 205 - 216

DOI: http://doi.org/10.1021/acsphotonics.7b00680

Copyright: © 2017 American Chemical Society

El acceso a la versión del editor puede requerir la suscripción del recurso
Access to the published version may require subscription

Polaritonic Chemistry with Organic Molecules

Johannes Feist,*,† Javier Galego,† and Francisco J. Garcia-Vidal*,†,‡

†*Departamento de Física Teórica de la Materia Condensada and Condensed Matter Physics Center (IFIMAC), Universidad Autónoma de Madrid, E-28049 Madrid, Spain*

‡*Donostia International Physics Center (DIPC), E-20018 Donostia/San Sebastian, Spain*

E-mail: johannes.feist@uam.es; fj.garcia@uam.es

Abstract

We present an overview of the general concepts of polaritonic chemistry with organic molecules, i.e., the manipulation of chemical structure that can be achieved through strong coupling between confined light modes and organic molecules. Strong coupling and the associated formation of polaritons, hybrid light-matter excitations, leads to energy shifts in such systems that can amount to a large fraction of the uncoupled transition energy. This has recently been shown to significantly alter the chemical structure of the coupled molecules, which opens the possibility to manipulate and control reactions. We discuss the current state of theory for describing these changes and present several applications, with a particular focus on the collective effects observed when many molecules are involved in strong coupling.

Keywords

polaritonic chemistry, photochemistry, organic molecules, quantum optics

1 Introduction

When the coherent energy exchange between a confined light mode and a quantum emitter becomes faster than the decay and decoherence of either constituent, the system enters into the regime of *strong coupling* or *vacuum Rabi splitting*.[1,2] The fundamental excitations of the system are then *polaritons*, hybrid light-matter excitations. This requires a large (collective) *Rabi frequency* $\Omega_R \propto \mu E_{1\mathrm{ph}}\sqrt{N}$, where N is the number of involved emitters, μ is their transition dipole moment, and $E_{1\mathrm{ph}} \propto V^{-1/2}$ is the electric field strength associated with one photon in the light mode (with V its effective mode volume). The figure of merit for a material is thus its dipole density $\mu^2 N/V$, with organic materials presenting a particularly favorable case due to their large dipole moments and high possible density. In addition, the large binding energies of Frenkel excitons in organic materials make them stable at room-temperature. This has allowed reaching the strong-coupling regime with a large variety of electromagnetic (EM) modes,[3] such as cavity photons,[4–8] surface plasmon polaritons,[9–12] surface lattice resonances,[13,14] and localized surface plasmons.[15,16] Typical Rabi frequencies range from ≈ 100 meV to more than 1 eV, a significant fraction of the uncoupled transition energy, for a wide range of organic materials such as dye molecules, J-aggregates, and even carbon nanotubes.[17,18] By using localized surface plasmon modes with extreme-subwavelength light confinement, recent experiments have achieved strong coupling at room temperature even down to the single-emitter level.[19–21]

The mixed light-matter character of organic polaritons enables a large number of interesting applications (see Ref. 22 for a recent review discussing polaritonic devices, including a comparison between organic and inorganic materials), such as polariton lasing and/or Bose-Einstein condensation[23–25] including nonlinear interactions,[26] long-range excitation transport,[27–30] and nonlinear optical response.[31,32]

While organic molecules favor polariton formation, they are not simple two-level quantum emitters, but rather have a complicated level structure including not only electronic excitations, but also rovibrational degrees of freedom. Most microscopic models for strong coupling treat

organic molecules as two-level systems (see Ref. 33 for a recent review), with some works modeling rovibrational degrees of freedom using effective decay and dephasing rates,[34] by allowing phonon-driven transitions between polaritons,[35,36] or by explicitly including a phononic degree of freedom[37–39] and examining its influence on the polariton properties. In 2012, a pioneering experiment by the group of Thomas Ebbesen showed that strong coupling could affect the rate of a photochemical reaction, photoisomerization from spiropyran to merocyanine.[40] Inspired by this result, polaritonic chemistry, i.e., the potential to manipulate chemical structure and reactions through the formation of polaritons (hybrid light-matter states) has become the topic of intense experimental[41–44] and theoretical research[45–56] in the past few years.

In this article, we first present an overview over the general concepts and theory of polaritonic chemistry with organic molecules, with some comparison of available theoretical approaches, in section 2. Afterwards, we discuss some specific examples of modifying photochemical reactions under single-molecule (section 3) and collective strong coupling (section 4). Here, we also demonstrate a novel type of collective conical intersection involving nuclear motion on separate molecules found within the *dark* states of the system, i.e., states that are not coupled to the light modes within a two-level approximation. The bulk of the article focuses on the single-excitation subspace that is relevant under linear response (i.e., not too strong driving) and provides general insight into the properties of polaritonic chemistry. However, in section 5, we discuss the double-excitation subspace and, in particular, examine correlation and effective interaction effects between polaritons, and their possible influence on chemical reactions.

2   General concepts

In this section, we present and extend the model for polaritonic chemistry that we developed over the last few years.[45,57,58] This fully quantum model describes a collection of organic

molecules strongly coupled to a confined light mode. It combines the concepts of quantum electrodynamics (QED), most notably quantized light modes, with those of quantum chemistry, such as potential energy surfaces (PES) that determine molecular structure and nuclear dynamics. This combination leads to the emergence of polaritonic PES (PoPES) determined by the energies of hybrid light-matter excitations.

A general molecule is described by the Hamiltonian

$$\hat{H}_{\mathrm{mol}} = \hat{T}_{\mathrm{n}} + \hat{H}_{\mathrm{e}}(\vec{R}), \tag{1}$$

where $\hat{T}_{\mathrm{n}}$ is the kinetic energy operator for the nuclei, while $\hat{H}_{\mathrm{e}}(\vec{R})$ is the electronic Hamiltonian, which contains all electronic contributions as well as the internuclear interaction, but only depends parametrically on the nuclear degrees of freedom, $\vec{R}$. Diagonalization of $\hat{H}_{\mathrm{e}}(\vec{R})$ yields a set $\{\Phi_k(\vec{R})\}$ of adiabatic electronic eigenstates, with $\hat{H}_{\mathrm{e}}(\vec{R})\Phi_k(\vec{R}) = V_k(\vec{R})\Phi_k(\vec{R})$, where the $V_k(\vec{R})$ are the electronic PES. The so-called Born-Huang expansion consists in writing the total system wavefunction in terms of this basis,

$$\Psi = \sum_k \chi_k(\vec{R})\Phi_k(\vec{R}), \tag{2}$$

where the nuclear wavefunctions $\chi_k(\vec{R})$ act as the expansion coefficients. Inserting this in the Schrödinger equation leads to

$$(\hat{T}_{\mathrm{n}} + V_k)\chi_k(\vec{R}) + \sum_{k'} \hat{\Lambda}_{k,k'}\chi_{k'}(\vec{R}) = E\chi_k(\vec{R}), \tag{3}$$

where the operator $\Lambda_{i,j} = \langle\Phi_i(\vec{R})|\hat{T}_{\mathrm{n}}|\Phi_j(\vec{R})\rangle - \hat{T}_{\mathrm{n}}\delta_{i,j}$ accounts for *nonadiabatic* coupling between electronic surfaces. These couplings become small for energetically well-separated PES, such that molecular dynamics can often be understood by considering nuclear motion on isolated PES and neglecting intersurface couplings, leading to the Born-Oppenheimer approximation. However, nonadiabatic couplings do become relevant when different PES

approach each other, especially close to conical intersections (points of degeneracy) which are known to determine many photochemical processes. For a more detailed analysis, see[59–63] and references therein.

We now extend the formalism discussed above to treat coupling of a collection of N molecules to one or several quantized light modes. The corresponding Hamiltonian includes a sum over bare-molecule Hamiltonians, the energy of the quantized light modes $\hat{H}_{\text{ph}}$, and the interaction between the molecules and the light modes $\hat{H}_{\text{int}}^{(i)}(\vec{R}_i)$. While they could be included easily, for simplicity we assume that direct interactions between the molecules are negligible. The total Hamiltonian is then given by

$$\hat{H}_{\text{tot}} = \sum_i^N \hat{T}_{\text{n}}^{(i)} + \sum_i^N \hat{H}_{\text{e}}^{(i)}(\vec{R}_i) + \hat{H}_{\text{ph}} + \sum_i^N \hat{H}_{\text{int}}^{(i)}(\vec{R}_i). \tag{4}$$

The Hamiltonian in this form is still completely general and can also be seen as an extension of the well-known Dicke or Tavis-Cummings models[64,65] to more complex emitters. It forms the starting point for almost all treatments of strong light-matter coupling involving molecules. For example, in the Holstein-Tavis-Cummings models,[39,47,48,52,66,67] nuclear motion is assumed to be described by harmonic oscillator potentials, which allows for trivial diagonalization of the full bare-molecule Hamiltonian (usually restricted to a single nuclear degree of freedom), and thus provides a convenient starting point for treatments of the strong-coupling regime. Another approach consists in extending density functional theory to also include photonic degrees of freedom, leading to quantum-electrodynamical density-functional theory.[46,53,68,69] The main challenge for practical applications of this powerful idea is the development of suitable functionals describing light-matter interaction based on the electron-photon density. In a related approach, the so-called Cavity Born-Oppenheimer approximation, the photon mode is described as a harmonic oscillator with "kinetic" and "potential" energy terms (corresponding to the electric and magnetic energy, respectively), which are then grouped with the corresponding molecular terms to obtain a Born-Oppenheimer description with an

additional formal "nuclear" degree of freedom corresponding to the photonic mode.[53,54]

Finally, the approach we follow here is based on the similarity between Eq. (4) and Eq. (1), and exploits that all contributions apart from the nuclear kinetic energy terms depend at most parametrically on the nuclear degrees of freedom. This allows the definition of an "electronic-photonic" Hamiltonian $\hat{H}_{e-ph}(\vec{q}) = \hat{H}_{tot} - \sum_i^N \hat{T}_n^{(i)}$, where $\vec{q} = (\vec{R}_1, \dots, \vec{R}_N)$ is the vector describing all nuclear coordinates of all molecules. Diagonalization of $\hat{H}_{e-ph}(\vec{q})$ then yields an adiabatic basis formed by polaritonic PES (PoPES). In Ref. 45, we introduced and explored this approach and the validity of performing the BOA within this setting, using a first-principles quantum approach that fully accounts for the electronic, nuclear, and photonic degrees of freedom on equal footing for a model molecule with restricted dimensionality. This work demonstrated that the PoPES provide a useful picture in the strong coupling regime, but that nonadiabatic effects can be important, especially for the upper excited states (i.e., the "dark" states and the upper polariton). It also showed that it is possible to diagonalize the electron-photon Hamiltonian in two stages, first for each molecule (e.g., using the well-known tools of quantum chemistry, or by exploiting simple analytical models), and then coupling only a relevant subset of states to the photonic modes.[49–51,57,58] It should be noted that in this approach, one obtains two types of nonadiabatic couplings between PoPES: those induced by the light-matter interaction, as well as the bare-molecule nonadiabatic couplings that have to be transformed into the new polaritonic basis. This formulation also allows for a straightforward interface to existing quantum chemistry methods, which can be used to calculate the bare-molecule structure at configuration $\vec{R}_i$ for each molecule separately. The light-matter coupling can then be treated within a small Hamiltonian involving only a few states per molecule, similarly as in existing excitonic models.[70,71] This effective decoupling between the "chemical" and "quantum optical" parts of the calculation allows the use of well-known approaches such as QM/MM (quantum mechanics/molecular mechanics) for treating big molecular systems.[72] Here, nuclear motion on the PoPES is treated classically, with nonadiabatic couplings introduced through surface hopping algorithms. The
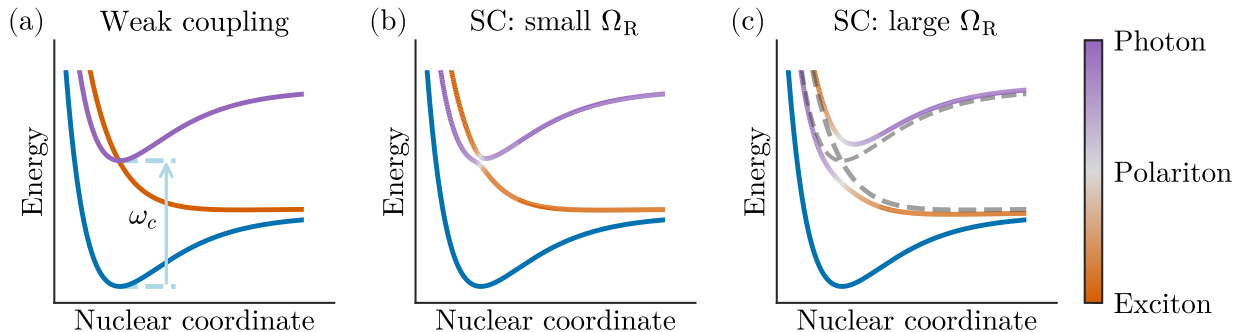
Figure 1: Conceptual potential energy surfaces for a single molecule and a light mode in (a) weak coupling and (b,c) strong coupling for different coupling strengths. The color represents the photonic fraction of the state from purely excitonic (orange) through polaritonic (light gray) to purely photonic (purple).

straightforward parallelizability of this approach has allowed the treatment of up to 1,600 Rhodamine molecules (within the single-excitation subspace) and their surrounding solvent, corresponding to 43,200 QM and 17,700,800 MM atoms in total, using 38,400 CPU cores in parallel.[72] However, this approach obviously requires considerable amounts of computing time, and due to the classical treatment of nuclear motion, the PoPES are only calculated "on the fly" and no structural information about the strongly coupled system is provided a priori. In the following, we focus on the general properties of PoPES and design strategies for achieving desired functionalities, based on simplified model molecules as in Refs. 57,58.

To demonstrate the general properties of PoPES, we first treat a minimal model involving a single molecule with two electronic states and one nuclear degree of freedom. The bare molecule is then characterized by its ground and excited PES, $V_g(q)$ and $V_e(q)$, respectively, which we here take to be similar to typical bound and dissociative PESs of diatomic molecules (blue and orange lines in Fig. 1a). We also assume that only the electronic transition is coupled to the light mode, which suffices to describe molecular excited-state processes, but cannot reproduce effects such as vibrational strong coupling.[73–75] Finally, the coupling to the electronic part is introduced within the dipole and rotating-wave approximations, such that the total number of electronic and photonic excitations is conserved, but the ultrastrong-coupling regime (where Rabi splittings become comparable to the transition

7

energies) cannot be treated (see Ref. 56 for an application of PoPES to ultrastrong coupling). The electronic-photonic part of the Hamiltonian then becomes

$$\hat{H}_{\text{e−ph}}(q) = V_g(q) + V_e'(q)\hat{\sigma}^\dagger\hat{\sigma} + \omega_c\hat{a}^\dagger\hat{a} + \vec{E}_{1\text{ph}} \cdot \vec{\mu}_{eg}(q)(\hat{a}^\dagger\hat{\sigma} + \hat{a}\hat{\sigma}^\dagger) \tag{5}$$

where $V_e'(q) = V_e(q) - V_g(q)$ is the position-resolved ground-to-excited-state excitation energy, $\hat{\sigma} = |g\rangle\langle e|$ is the molecular electronic transition operator, ω_c is the confined photon frequency, and $\hat{a}$ is the bosonic photon annihilation operator. The exciton-photon interaction is determined by $\vec{E}_{1\text{ph}}$, the single-photon electric field strength of the confined light mode, and $\vec{\mu}_{eg}(q)$, the (configuration-dependent) electronic transition dipole moment between the ground and excited states. Diagonalization of $\hat{H}_{\text{e−ph}}(q)$ then yields the adiabatic PoPES of the coupled light-matter system.

When the coupling is negligible (Fig. 1a), two clearly distinguishable excited states exist: the molecular exciton, characterized by the excitonic PES (orange line), and the state corresponding to a photon in the light mode, with the molecule in its ground state (giving a copy of the ground-state PES shifted up by the photon energy ω_c, purple line). As the coupling is increased (Fig. 1b,c), these two surfaces hybridize in regions close to resonance, resulting in new polaritonic PES with mixed light-matter character, as codified by the color scale measuring their photon component $n_{ph} = \langle\hat{a}^\dagger\hat{a}\rangle$, spanning from orange (bare exciton) through light gray (polariton) to purple (bare photon). Already in this simple example, it becomes clear that the PoPES have significantly different shapes than the PES of the uncoupled system, i.e., that strong coupling can influence the molecular structure. In addition, the presence of crossings between the two types of excited states in the uncoupled system (which become higher-dimensional seams when more than one nuclear degree of freedom is involved) immediately suggests that strong coupling could lead to the emergence of new, cavity-induced nonadiabatic transitions and conical intersections.[45,49,57] It should be noted that these effects are strongly reminiscent of the changes in molecular structure observed

under illumination with intense laser pulses.[76–81] However, while these approaches rely on the presence of many photons in the light field to achieve strong interactions, strong-coupling induced modifications appear due to *vacuum Rabi splitting*, where the field associated with a single photon becomes sufficiently strong to change the molecular structure even when no external driving at all is present.

For simplicity, we have neglected dissipative processes such as decay and dephasing here and in the following sections. For organic polaritons, these processes can either originate from the molecules or from the photonic modes. In most current experiments, the photonic modes show very fast decay, with typical lifetimes on the order of tens to hundreds of femtoseconds.[4,13,16,20,82] This is an intrinsic limitation in metallic structures (with strong absorption in the visible), but can be mitigated somewhat by working at lower transition frequencies in the near-infrared where metal reflectivities become larger.[32] In contrast, wavelength-scale dielectric structures such as Fabry-Perot or photonic crystal cavities can in principle be engineered with long lifetimes on the order of tens of picoseconds,[83,84] or even above nanoseconds for whispering gallery mode resonators.[85] Reactions in polaritonic chemistry that rely on relatively long excited-state lifetimes could thus benefit from the use of such photonic structures. Regarding the molecular part, the intra-molecular vibrational degrees of freedom and interactions with the host or solvent typically lead to effects on a variety of timescales, such as (essentially static) inhomogeneous broadening, but also relatively fast vibrational relaxation, dephasing, and nonradiative decay through conical intersections, with timescales on the order of hundreds of femtoseconds to picoseconds.[60,61,86] However, these processes take place on the PES of the system, and can thus in principle be described within the framework of polaritonic chemistry (as, e.g., done in Ref. 72, where the solvent molecules are represented through molecular mechanics, i.e., with interactions given by classical force fields). The intrinsic linewidth of the PoPES is then given only by their (free-space) radiative decay, which is determined by the dipole transition matrix element and leads to lifetimes on the order of nanoseconds even for good emitters. Since the photonic contribution to the

9

polariton decay depends strongly on the actual system, and the molecular contribution can in principle be treated within the framework, we thus mostly neglect them in the current text, which aims to give a general introduction to the concepts of polaritonic chemistry. However, more detailed treatments of dissipation processes both in the photonic and in the molecular parts of polaritonic systems will certainly be beneficial to a complete understanding of such systems and in particular, the limitations of experimental implementations.

3   Single-molecule polaritonic chemistry

In the previous section, we introduced the concept of PoPES and showed the possibility that strong coupling offers of influencing the excited-state energy landscapes of molecular systems. In this section, we describe two examples of single-molecule strong coupling leading to significantly modified chemical reaction dynamics. In addition to providing valuable insight into the fundamental properties of polaritonic chemistry, single-molecule strong coupling has recently entered the realm of experimental feasibility, with several experiments reporting strong coupling down to the single-emitter level at room temperature within the last year.[19–21]

The two molecules we treat are again represented through restricted models describing nuclear motion along a single reaction coordinate on two electronic PES. In the first case (previously studied in Ref. 58), we demonstrate the possibility of significantly increasing the quantum yield of a photochemical reaction, while in the second case (taken from Ref. 57), we strongly suppress the reaction. In the first case, the bare-molecule level structure (shown in Fig. 2a) is similar to that of molecules proposed for solar energy storage.[87–89] It consists of a ground state PES with two minima representing a stable and a metastable nuclear configuration, respectively, as well as a relatively flat excited-state PES. In this model, the excited-state minimum is energetically well-separated from the ground-state maximum, so that nonadiabatic couplings are small and excited-state wavepackets survive long enough to thermalize through interactions with low-frequency molecular vibrations and external bath
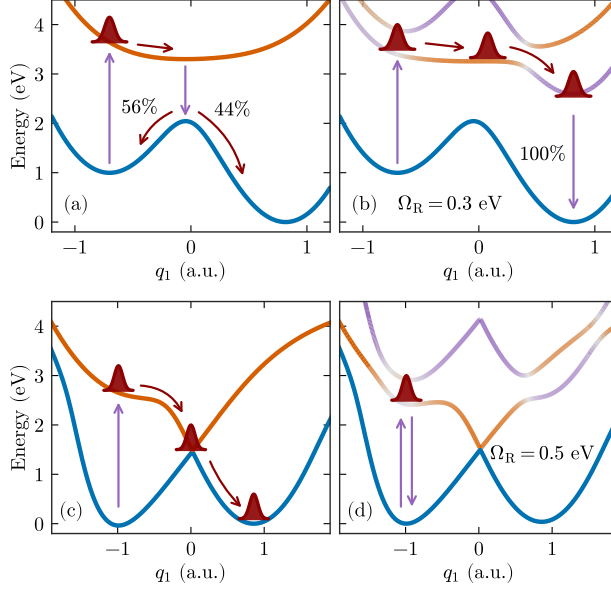
10

Figure 2: Polaritonic potential energy surfaces of two model molecules in weak and strong coupling. (a,c) Bare molecules without light-matter interaction. (c,d) Strongly coupled molecules, with (b) $\Omega_R = 0.3$ eV and (d) $\Omega_R = 0.5$ eV (photon energy $\omega_c = 2.65$ eV in both cases). The color scale is identical to Fig. 1.

modes, which happens on typical timescales of picoseconds. We study the back-reaction (schematically indicated in Fig. 2a), with the molecule initially in the metastable left-hand minimum (corresponding to stored vibrational energy of around 1 eV). Absorption of a photon then creates a wavepacket at the same position on the electronically excited PES, from where it relaxes to the local minimum. From there, it can decay (either radiatively or nonradiatively) to the ground state. The ground-state nuclear wavepacket is then well-approximated by a projection of the relaxed excited-state wavepacket onto the ground-state PES. In the further propagation, this wavepacket splits, with roughly half (56%) returning to the metastable isomer and half (44%) going to the stable isomer on the right-hand side. This corresponds to a photochemical quantum yield of 0.44 for this energy-releasing back-reaction.

In Fig. 2b, we show the PoPES generated by bringing a single such molecule into strong coupling with a quantized light mode. The lower-energy PoPES corresponds to a mix between the ground-state-like photonically excited PES and the molecular excited PES, with a minimum at the stable ground-state configuration. For the parameters chosen here,

there are no barriers along the PoPES on the path from the metastable configuration to the stable one. An excited wavepacket would thus vibrationally relax to this minimum, with its character along the way changing from a polaritonic excitation at first to a mostly excitonic one, then back to a polaritonic one, and finally to an almost purely photonic excitation. The system would thus decay through radiative relaxation by emission of the photon with very high probability, leaving the molecule in the stable configuration with a corresponding reaction quantum yield approaching 100%. This phenomenon is described in Ref. [58] in more detail, where it is also shown that under collective strong coupling, the process described here can repeat multiple times in different molecules after just a single excitation, corresponding to triggering a many-molecule reaction with just a single photon. The reaction quantum yield then far exceeds unity, such that polaritonic chemistry could provide a strategy to overcome the second law of photochemistry.[90]

Following our previous work,[57] we next analyze a model molecule that undergoes rapid isomerization after absorption of a photon. Photoisomerization is a class of photochemical reactions of great importance in many biological systems,[91,92] and is also relevant for an extensive range of technological applications such as memories, switches, actuators, or solar cells.[93–95] We study a simplified model molecule that can represent a wide range of photoisomerization reactions, such as *cis-trans* reactions in stilbene, azobenzene or rhodopsin (rotations around C=C or N=N bonds), with an electronic structure depicted in Fig. 2c. We again consider a single nuclear reaction coordinate, while orthogonal nuclear degrees of freedom are considered to be fully relaxed. The ground state has two minima, each representing one stable isomer, at $q = q_0 \approx -1.05$ a.u. and $q \approx 1$ a.u. The system displays a narrow avoided crossing at $q \approx 0$ that allows for efficient nonadiabatic coupling between the ground and excited PES, $V_g(q)$ (blue line) and $V_e(q)$ (orange line), respectively. The ground-excited transition dipole moment has the shape $\mu_{eg}(q) \propto \arctan(q/q_\mathrm{m})$, with $q_\mathrm{m} = 0.625$ a.u., in order to represent the sudden polarization effect occurring near nonadiabatic transitions,[96] although the specific shape of $\mu_{eg}(q)$ does not strongly affect the results presented here.

In the bare molecule, excitation from the left-hand (stable) ground-state minimum again produces a nuclear wavepacket on the electronically excited PES, which in this case rapidly reaches the narrow avoided crossing where it undergoes efficient nonradiative decay to the ground-state PES and continues propagating to the right-hand side minimum of the ground state. This process is very fast, with typical timescales of a few hundred femtoseconds.[92] After bringing the system into strong coupling, this picture changes drastically. The lower PoPES, being a mixture of the ground and excited-state surfaces, can be made to possess a minimum close to the initial position, with a potential energy barrier preventing the initial nuclear wavepacket motion towards the nonadiabatic crossing (see Fig. 2d). For this molecule, it is thus possible to efficiently suppress a photochemical reaction through strong coupling. In the next section, we discuss collective effects under strong coupling involving many molecules and, in particular, demonstrate that these can lead to an even more efficient suppression of photochemical reactions.

4   Collective effects

In this section, we treat the effects found when strong coupling is achieved through collective coupling, i.e., the coherent interaction of many molecules with the same light mode. As already discussed above, this leads to an electronic-photonic Hamiltonian that depends parametrically on $\vec{q} = (\vec{R}_1, \ldots, \vec{R}_N)$, i.e., on the nuclear degrees of freedom of all involved molecules. This general property is inherited by the associated PoPES, and implies that the effective intermolecular interaction induced by strong coupling could lead to novel correlations between nuclear motion on different molecules. Stated differently, collective strong coupling can be seen as leading to the formation of a "supermolecule" spanning all coupled molecules. In the following, we show that this indeed offers a range of new phenomena that further enhance our ability to control the dynamics and chemistry of a molecular ensemble. In particular, we will discuss the *collective protection* effect, one of the central features of collective strong

coupling, in some detail.

For simplicity, we again assume that the molecules are described by only two electronic states, and in addition we take all molecules to be coupled equally to the photonic mode. The Hamiltonian is then a straightforward extension of Eq. (5) to include sums over the molecules. Since we will study cuts where several molecules have the same configuration (e.g., we will assume that most molecules are in the equilibrium position), we can significantly reduce the size of the associated Hilbert space by introducing collective spin operators[64,97]

$$\hat{S}_+^\alpha = \sum_{i_\alpha=1}^{N_\alpha} \hat{\sigma}_{i_\alpha}^\dagger \quad \text{and} \quad \hat{S}_-^\alpha = \sum_{i_\alpha=1}^{N_\alpha} \hat{\sigma}_{i_\alpha}, \tag{6}$$

where $\hat{\sigma}_i$ correspond to the single-emitter operators for molecule i already used above and α labels groups of molecules with the same configuration $\vec{R}_{i_\alpha} \equiv \vec{R}_\alpha$ (with $\sum_\alpha N_\alpha = N$). The single-molecule two-level operators are formally identical to spin-1/2 operators, such that the collective operators $\hat{S}_\pm^\alpha$ are spin-$N_\alpha/2$ operators.[97] We can thus extend Eq. (5) as

$$\hat{H}_{\text{e-ph}}(\vec{q}) = V_G(\vec{q}) + \sum_\alpha V_e'(\vec{R}_\alpha)\hat{n}_\alpha + \omega_c \hat{a}^\dagger \hat{a} + \vec{E}_{\text{1ph}} \cdot \sum_\alpha \vec{\mu}_{eg}(\vec{R}_\alpha)\left(\hat{a}^\dagger \hat{S}_-^\alpha + \hat{a}\hat{S}_+^\alpha\right), \tag{7}$$

where $V_G(\vec{q}) = \sum_i V_g(\vec{R}_i)$, and $\hat{n}_\alpha = \sum_{i_\alpha} \hat{\sigma}_{i_\alpha}^\dagger \hat{\sigma}_{i_\alpha} = \hat{S}_z^\alpha + N_\alpha/2$ is the excitation number operator for group α (with $\hat{S}_z^\alpha$ the z-component of the collective spin operator). Since the Hamiltonian now contains only collective molecular operators, the electronic-photonic states can be expressed in the collective spin basis $\hat{n}_\alpha|n_\alpha\rangle = n_\alpha|n_\alpha\rangle$ (for convenience, we use $n_\alpha = m_\alpha + N_\alpha/2$ as the quantum number, where m_α is the z-component of the spin), which leads to a significant reduction of the Hilbert space. Within the single-excitation subspace, the savings afforded by this approach are not essential unless N becomes very large, as even the size of the "naive" molecular Hilbert space only scales linearly with N. However, if more than one excitation is allowed (as we will discuss below in section 5), the size rapidly explodes and the collective approach enables treatment of systems that would otherwise be unreachable. For example, the full Hilbert space for the molecular part scales as 2^N for the
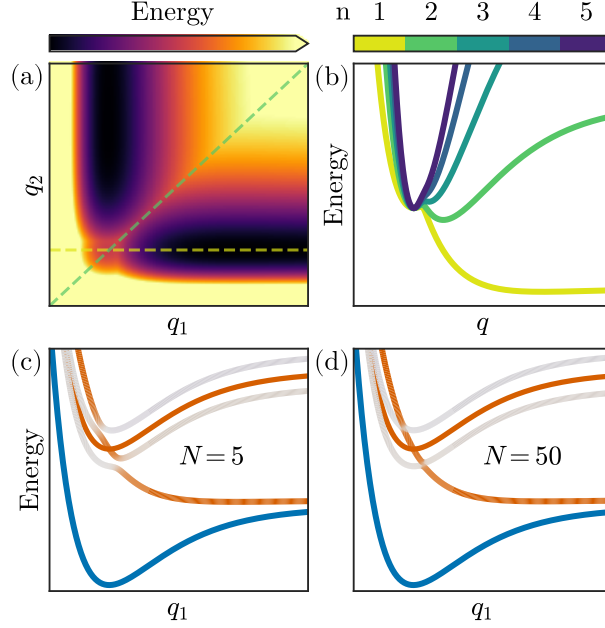
14

Figure 3: Collective dynamics in the single-excitation subspace. (a) Lowest excited two-dimensional PoPES for motion of two molecules out of $N = 50$ molecules. (b) Lowest excited PoPES for correlated simultaneous motion of $n = 1, \ldots, 5$ molecules (for $N = 50$). (c,d) Full PoPES for motion of one molecule for the case of (c) $N = 5$ molecules and (d) $N = 50$ molecules, with identical color scale as in Fig. 1.

"naive" approach, but as $\prod_\alpha (N_\alpha + 1)$ when using collective states (the product of the Hilbert spaces of spins $N_\alpha/2$ with $N_\alpha + 1$ distinct states). This savings comes from the fact that the collective basis only includes bright states, superpositions of molecular excitations that couple to the photonic mode, but excludes uncoupled dark states from the Hilbert space.

We start by analyzing collective strong coupling for the simple model molecule depicted in Fig. 1, and restrict ourselves to the single-excitation subspace. We initially take a cut where 2 molecules move, with the remaining $N - 2$ molecules fixed in the equilibrium position q_{eq} (the minimum of the ground state PES $V_g(q)$). Fig. 3a shows the corresponding lowest excited PoPES for $N = 50$ and Rabi frequency $\Omega_R = 0.3$ eV. Simple inspection already reveals that globally, the lowest excited PoPES here is not an independent sum of single-particle potentials $V_{LP}(q_1, q_2, \ldots) \neq \sum_i v_i(q_i)$, i.e, that strong coupling implies some correlation between the nuclear motion of different molecules.[45] In addition, the chosen cut here shows a general feature that aids in the analysis of these high-dimensional surfaces: While motion of only a

15

single molecule at a time (dashed yellow line in Fig. 1a) only shows a small barrier towards dissociation, motion of multiple molecules at the same time (green dashed line along the diagonal in Fig. 3a) results in a high potential energy barrier. This can be understood easily: There is only a single excitation in the system, such that motion for all but one molecule proceeds along a ground-state like surface for all uncoupled states, which introduces a barrier for deviations from the equilibrium position. This feature of the uncoupled states is necessarily reflected also in the PoPES, and suppresses motion of several molecules at a time. To confirm this, in Fig. 3b we show the lowest excited PoPES for concerted motion of between 1 and 5 molecules, which very quickly leads to a significant barrier that increases with the number of comoving molecules. This implies that for many typical molecules with locally stable ground states, motion on the lowest excited PoPES after photon excitation will proceed mostly along a cut corresponding to motion of a single molecule, significantly simplifying the analysis.

We thus turn to the full excited-state spectrum, with motion restricted to just a single molecule. The uncoupled excited-state surfaces then consist of N surfaces that follow the ground-state PES along q_1 (the photonically excited PES and $N-1$ surfaces where a molecule at the equilibrium position is excited), as well as one surface where the moving molecule is excited and the PES thus follows $V_e(q_1)$. In Fig. 3c,d, the resulting PoPES are shown for $N = 5$ and $N = 50$ molecules, respectively (while keeping the Rabi frequency fixed). As in Fig. 1, the color scale again encodes the excitonic/polaritonic/photonic nature of the state. It can be seen that the polaritonic parts (in light gray) of the PoPES approximately follow the shape of the ground state PES. This can be understood by the fact that in polaritonic states, a single excitation is coherently distributed over all molecules and the light mode, and nuclear motion is thus mostly determined by the ground-state PES. This effect can be seen as a generalization of the so-called "polaron decoupling" found in Holstein-Tavis-Cummings models[39,48,52,66] (where nuclear degrees of freedom are restricted to harmonic oscillator motion) to arbitrary PES. This effect is also well-known for molecular J- and

H-aggregates, where an excitation is distributed over many molecules not due to coupling with a confined light mode, but due to direct intermolecular interactions.[98] As in molecular aggregates, the similarity between the ground-state PES and the lowest excited PoPES also implies that optical transition lineshapes should be significantly narrower compared to a bare molecule due to the fact that the Franck-Condon factors become approximately diagonal if the excited PoPES is ground-state-like in a large enough region around the equilibrium position.

We next study the avoided crossing between a purely excitonic PES and a polaritonic one that is seen for q_1 slightly larger or smaller than the equilibrium position in Fig. 3c,d. This avoided crossing is clearly seen to become much sharper as the number of molecules is increased. The crossing occurs since the excited molecule has moved sufficiently to fall out of resonance with the photonic mode, but then becomes resonant with the polariton formed by the remaining $N-1$ molecules and the photon. Using a diabatic basis based on these ingredients reveals that the effective coupling becomes proportional to the single molecule-photon coupling, which scales as $\sim N^{-1/2}$ for the chosen case of the collective Rabi frequency being independent of N (corresponding to a molecular material with constant density coupled to photonic modes with different effective mode volumes). This reduction in coupling can be understood as the distributed excitation having to collapse onto a single molecule, or equivalently by interpreting the polariton involving the $N-1$ other molecules as simply a shifted photonic mode coupling to the single-molecule exciton at this position. In any case, this reduction in coupling constitutes the second aspect of *collective protection* that stabilizes polaritonic excitations chemically. It should be noted, however, that while we study motion of just one molecule here, the symmetries of the system dictate that *any* one of the N molecules could move, partially offsetting the reduced coupling.

Finally, these considerations also suggest some general design principles for obtaining a desired functionality through polaritonic chemistry. In particular, the excited-state PoPES can be obtained by "cutting and pasting" ground-state-like (polaritonic) parts of the surface
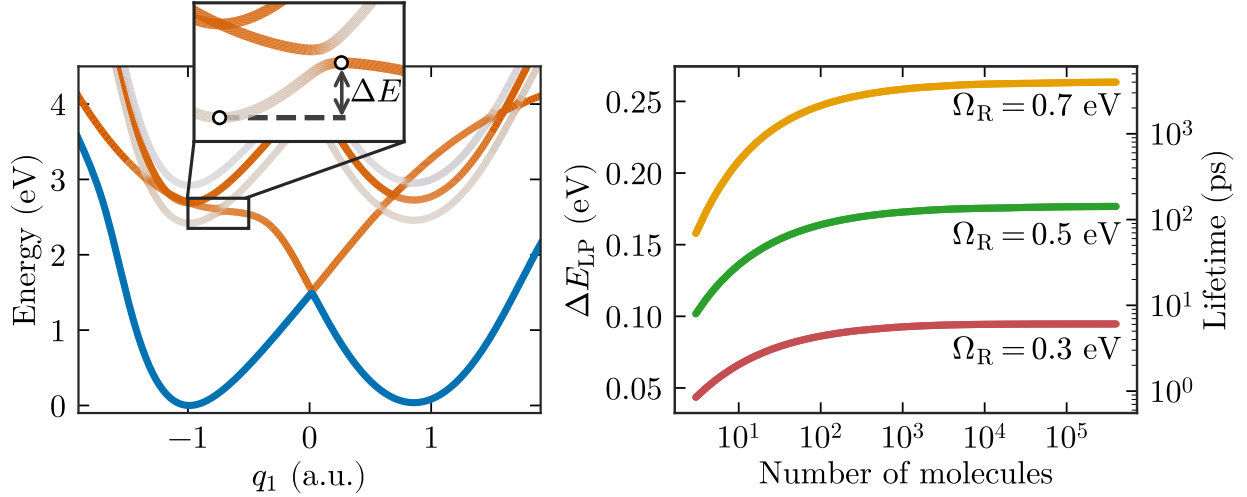
17

Figure 4: Collective protection effects: (a) PoPES for $N = 50$ molecules in strong coupling, one of which can move while the rest are frozen in their equilibrium position. The inset shows a zoom to the region where the effect of collective protection is most clearly seen. (b) Energy barriers vs number of molecules for different values of Rabi splitting. The right axis shows the equivalent lifetime predicted through transition state theory.

together with exciton-like parts, with the details determined by the coupling strength and photonic mode frequency in addition to the bare-molecule structure.

4.1 Supressing photochemical reactions

In this section, we illustrate how it is possible to take advantage of the collective protection effect to almost completely suppress a photoisomerization reaction, as first demonstrated in.[57] We use the same molecular model as in Fig. 2c,d, but now for the case of N molecules coupled to the same cavity mode. Fig. 4a shows the corresponding PoPES for $N = 50$ molecules, again concentrating on motion of only one molecule with all others in the equilibrium position. For the model considered here, the ground-state-like region of the lowest PoPES is sufficiently extended to provide a well-defined local minimum with a significant potential energy barrier ΔE (see inset in Fig. 4a) towards the surface leading to isomerization. As discussed above, optical excitation from the ground state to the lowest PoPES will mostly proceed to the lowest vibrational state, so that initially no motion takes place. The wavepacket can then

thermalize (on typical timescales of picoseconds at room temperature), with the lifetime for passing over the barrier determined by the probability of gaining enough energy from the bath to overcome the barrier. While a detailed calculation of this lifetime is outside the scope of this paper, we here obtain an estimate based on transition state theory.[99] This estimate should be taken with some caution, as there are at least two features of the polaritonic system considered here that differ from the situation treated by standard transition state theory: For one, there is not just an energetic barrier that has to be overcome, but, as discussed above, the top of the barrier corresponds to an increasingly narrow avoided crossing as N is increased, with the splitting there scaling as $1/N$. Within a diabatic picture, this corresponds to a transition probability to the excitonic PES that also scales as $1/N$. At the same time, there is not a single barrier, but N identical barriers for motion of any one of the molecules (with all others close to equilibrium). This gives an enhancement by a factor of N, and the two effects discussed approximately cancel each other. We thus assume that transition state theory provides a useful estimate of the excited state lifetime, which gives the following relation between the energy barrier height ΔE of the potential well and the lifetime τ within it:

$$\tau \approx \frac{h}{k_{\mathrm{B}}T} \exp\left(\frac{\Delta E}{k_{\mathrm{B}}T}\right), \tag{8}$$

where $k_{\mathrm{B}}T \approx 25.9$ meV at room temperature. Under the condition that the photon frequency is fixed to stay close to resonance at the equilibrium position, the barrier height in the lowest PoPES depends on two parameters: the Rabi frequency and the number of molecules. Their combined effect on ΔE is shown in Fig. 4b, which demonstrates that increasing N leads to higher barriers, with the value saturating for a given Rabi splitting at around $N = 100$. Alternatively, larger Rabi frequencies and the associated reduction in the minimum energy of the lowest PoPES lead to effectively higher barriers and thus a more efficient suppression of the photoisomerization reaction. The associated lifetimes (shown on the right axis in Fig. 4b) range from about one picosecond to about 10 nanoseconds depending on parameters. The final fate of an excited wavepacket will thus depend on the competition between two
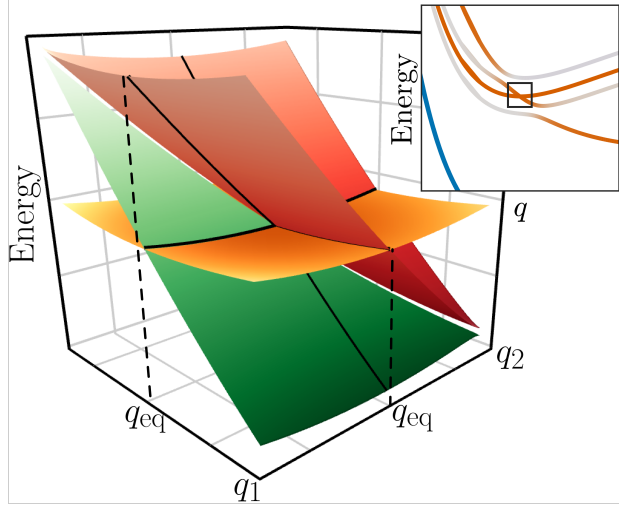
Figure 5: Zoom on the collective light-induced conical intersection between dark state PoPES under motion of two molecules.

timescales: that of the vibrational wavepacket trapped inside the local potential well in the lower PoPES, as well as that of the polaritonic state against relaxation, typically dominated by the photonic fraction of the polariton. As discussed at the end of section 2, this can range from tens of femtoseconds to picoseconds or more.

4.2   Dark-state collective conical intersections

As a second example of collective effects induced by strong coupling, we focus in more detail on the mostly excitonic regions of the PoPES close to the bare-molecule excitation energy at equilibrium. When all molecules are in the same configuration there are $N-1$ so-called "dark" states, superpositions that do not couple to the photonic mode, at the energy of the bare exciton. When nuclear motion is considered, this corresponds to $N-1$ PoPES becoming degenerate exactly at this point, but these degeneracies are lifted for motion along any nuclear degree of freedom. A zoom into the region close to the point of degeneracy is shown in Fig. 5 for motion of two molecules. Here, the two sloped surfaces (green and red) roughly correspond to motion of the single-molecule excited PES of each of the two molecules, while the orange horizontal surface corresponds to the remaining $N-3$ degenerate dark

PES. Along the seams where this surface crosses the two sloped surfaces, $N-2$ surfaces are degenerate. The structure discussed here thus gives rise a to high-dimensional hierarchy of hyperdimensional surfaces where between 2 and $N-1$ PoPES become degenerate, i.e., conical intersection seams of different dimensionality.[60,61,63]

Here, it should be noted that these intersections do not correspond simply to intersections of completely decoupled surfaces, but that they actually show non-zero coupling away from the point of intersection (see, e.g., along the diagonal $q_1 = q_2$ in Fig. 5). This interaction is due to the cavity, as the approximate dark states are not completely dark anymore if the perfect degeneracy between emitters is lifted. At the same time, the very small coupling to the cavity implies that the resultant electronic-photonic states are almost purely excitonic and their intrinsic linewidth due to radiative decay is small, similar to the bare molecules (with lifetimes on the order of nanoseconds), even within lossy cavities. One particularly interesting detail here is that these conical intersections necessarily describe nuclear motion of spatially separated molecules. They thus provide another example of collective strong coupling inducing potentially nontrivial correlated nuclear dynamics between different molecules, validating the concept of a "supermolecule" formed from all molecules through collective strong coupling. It should also be noted that the occurrence of this structure is quite robust against inhomogeneous broadening, i.e., energy shifts of the transition energies of the different molecules. This just leads to slight shifts of the nuclear positions where the different molecular PES become degenerate, but does not destroy the topology

5   PoPES in the two-excitation subspace

Up to now, we have only discussed the PoPES within the zero- and single-excitation subspace. While this is the subspace probed under weak excitation (linear response) in experiment, the nonlinear response of polaritonic systems is a topic of great current interest. It becomes relevant in, among others, transient absorption measurements,[40,100] nonlinear optics
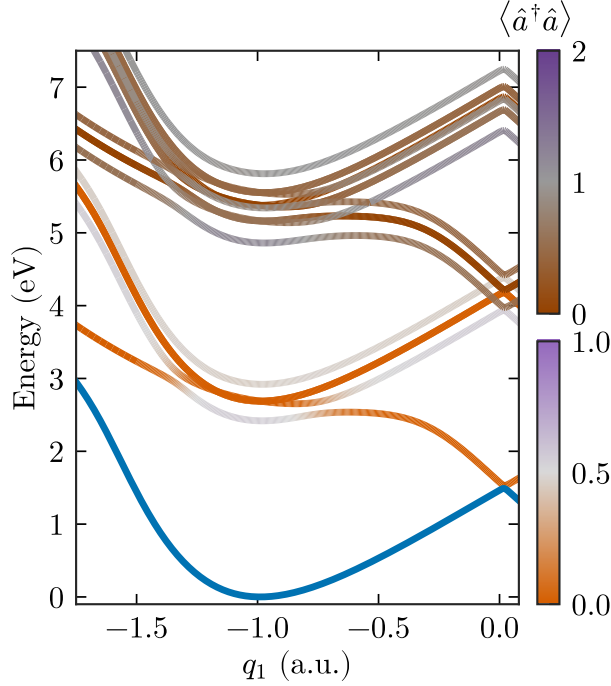
Figure 6: PoPES up to the two-excitation subspace for the model molecule of Fig. 2(c,d). The two color scales indicate the photon fraction in the single- and two-excitation subspace, respectively.

setups,[31,32,101] and studies of polariton lasing and condensation.[13,23–26] We here focus on the two-excitation subspace and investigate whether we still observe the collective protection effect, and whether we observe any effective polariton-polariton interactions leading to correlated motion. As in the rest of the manuscript, we neglect direct dipole-dipole interactions between the molecules, such that saturation is the only source of nonlinearities or effective polariton-polariton interactions (as typically observed in organic-based polaritonic systems due to the localized nature of Frenkel excitons[23]). When the number of molecules is much larger than the number of excitations, it is expected that the system bosonizes, i.e., that the response becomes linear and polaritons become approximately independent of each other.[102] However, it has recently been found that nonlinearities can survive even for surprisingly large values of N under strong coupling conditions.[103] As mentioned above, the use of collective spin operators becomes essential for the computational treatment in this case, as it keeps the problem easily tractable even for relatively large numbers of molecules (where a naive
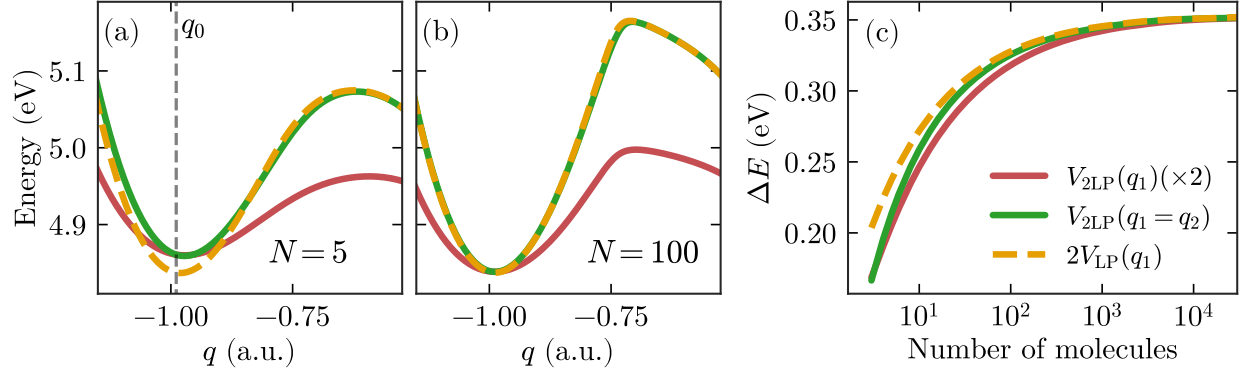
Figure 7: (a,b) Comparison of the PoPES in the double-excitation subspace for motion of one molecule (red line) and two molecules (green line), and twice the lower PoPES in the single-excitation subspace for motion of one molecule (orange dashed line), for $N = 5$ and $N = 100$ coupled molecules, respectively. (c) Dependence of the energy barrier for double photoisomerization with the number of molecules for the reaction paths corresponding to the PoPES in (a,b).

approach would scale with N^2).

We use the molecular model for which we found suppression of photochemical reactions and calculate the PoPES for up to two excitations with $N = 50$, shown in Fig. 6. The large number of surfaces seen in the two-excitation subspace can be approximately qualified within an independent-particle picture (expected to be exact in the limit $N \to \infty$), corresponding to, for example, excitation of 2 lower polaritons, or one lower and one upper polariton. The color scale within the two-excitation subspace again measures the photonic contribution to each state, now spanning from $\langle n_{ph} \rangle = 0$ (two excitons, dark orange) through dark gray (one exciton, one photon) to $\langle n_{ph} \rangle = 2$ (two photons, dark purple).

In the following, we will focus on the lowest PoPES within the two-excitation manifold, which we label as $V_{2LP}(q_1, q_2, \dots, q_N)$ as it corresponds approximately to two lower polaritons close to equilibrium. Note that for the two-state molecules considered here, isomerization after double excitation (i.e., after absorption of two photons) in the uncoupled system corresponds to two independent excitons on separate molecules, with motion proceeding on the surface $V_{2e}(q_1, q_2) = V_e(q_1) + V_e(q_2)$. This implies that, in contrast to the single-excitation subspace, concerted motion of two molecules (e.g., along $q_1 = q_2$) is not a priori suppressed under strong

23

coupling. In the limit $N \to \infty$, the lowest surface should again support independent motion, but now on polaritonic surfaces. Consequently, a cut where only two molecules move should approximately fulfill $V_{2LP}(q_1, q_2, q_{eq}, \ldots, q_{eq}) \approx V_{LP}(q_1) + V_{LP}(q_2)$.

This is studied in Fig. 7, which shows two cuts through V_{2LP}, one in which only q_1 is varied (red solid line) and one in which $q_1 = q_2$ are varied together (green solid line). In addition, it shows the independent-particle limit of $2V_{LP}(q_1)$ (dashed yellow line). In all three cases, all remaining molecules are fixed to the equilibrium position. The plots are restricted to the region of interest $q \lesssim -0.5$ a.u., with subplots showing the cases $N = 5$ (a) and $N = 100$ (b). For the case of $N = 5$ molecules, it is clearly visible that simultaneous motion of two molecules has a slightly lower barrier than would be expected in the independent-particle limit due to a noticeable blueshift around the equilibrium position, indicating saturation-induced effective polariton-polariton interactions. These differences disappear for large enough N and are barely visible for the case $N = 100$ shown in Fig. 7b.

In order to clearly distinguish whether simultaneous motion of several molecules is favored compared to the independent-particle limit, we now directly compare the barrier heights for two-molecule reactions for the different cases studied here in Fig. 7c. Each line corresponds to the same case in Fig. 7a,b, with the difference that the energy barrier ΔE for motion of one molecule in the two-excitation subspace has been multiplied by 2 for the sake of comparison. As expected, all correlations disappear for large numbers of molecules, with the barrier heights converging to the same value. However, even for a considerable number of molecules such as $N = 100$ the correlations are non-negligible (remember that transition rates depend exponentially on barrier height, Eq. (8)), suggesting that polaritonic chemistry could possess subtle non-bosonic response even for mesoscopic numbers of molecules, similarly as recently found for photon correlations.[103] In particular, for the model studied here, the barrier for simultaneous motion of two molecules after double excitation of the system $V_{2LP}(q_1, q_2)$ is slightly smaller than expected from an independent-particle model $(2V_{LP}(q_1))$. Interestingly, motion of just a single molecule in the two-excitation subspace is even less suppressed, with

24

the barrier consistently less than twice as high. It should be noted that the subtle effects found for the specific model discussed here will of course be challenging to measure experimentally, but they could point a way towards more pronounced polariton-polariton interaction effects in polaritonic chemistry.

6 Summary and Outlook

In conclusion, we have presented an overview of the theory of polaritonic chemistry under strong light-matter coupling, based on the concept of polaritonic potential energy surfaces (PoPES). For the experimentally most relevant case of collective strong coupling, the general properties of "collective protection" lead to PoPES that can be understood to arise from a "cut & paste" operation combining ground-state-like polaritonic and excited-state-like excitonic surfaces. This implies a wide range of freedom for the design of novel surfaces, allowing to manipulate the photophysics and photochemistry of the involved molecules. We illustrated these concepts using several examples on the single-molecule and many-molecule level, and furthermore demonstrated a high-dimensional nested structure of collective conical intersections with varying amount of degeneracy induced in the dark states of the system. Finally, we showed that under multiple excitation, saturation effects leading to effective polariton-polariton interactions can influence the molecular dynamics, with correlations and deviations from an independent-particle picture even for relatively large numbers of molecules.

We expect that over the next few years, the potential of polaritonic chemistry will be further explored. In particular, there is a need for more experiments to verify and challenge the existing theoretical predictions. In terms of theory, there are several initiatives underway to allow the treatment of more and more complex systems, which should also allow easier comparison to forthcoming experiments. In the long term, a goal of the field will certainly be to investigate the use and applicability of polaritonic chemistry for practical applications. Such applications could include the catalysis of reactions for which no conventional catalyst

is known, or to do so cheaper and/or with less pollution than conventional catalysts. Another possible application is in future (room-temperature) quantum technologies exploiting the hybrid light-matter nature of organic polaritons, where the tools of polaritonic chemistry could help in controlling and tuning the properties of the polaritons, and possibly even to exploit chemical reaction dynamics for quantum technology applications.

Acknowledgement

References

(1) Thompson, R. J.; Rempe, G.; Kimble, H. J. Observation of normal-mode splitting for an atom in an optical cavity. *Phys. Rev. Lett.* **1992**, *68*, 1132.

(2) Weisbuch, C.; Nishioka, M.; Ishikawa, A.; Arakawa, Y. Observation of the coupled exciton-photon mode splitting in a semiconductor quantum microcavity. *Phys. Rev. Lett.* **1992**, *69*, 3314.

(3) Törmä, P.; Barnes, W. L. Strong coupling between surface plasmon polaritons and emitters: a review. *Rep. Prog. Phys.* **2015**, *78*, 013901.

(4) Lidzey, D. G.; Bradley, D. D. C.; Skolnick, M. S.; Virgili, T.; Walker, S.; Whittaker, D. M. Strong exciton-photon coupling in an organic semiconductor microcavity. *Nature* **1998**, *395*, 53.

(5) Lidzey, D. G.; Bradley, D. D. C.; Armitage, A.; Walker, S.; Skolnick, M. S. Photon-Mediated Hybridization of Frenkel Excitons in Organic Semiconductor Microcavities. *Science* **2000**, *288*, 1620.

(6) Kéna-Cohen, S.; Davanço, M.; Forrest, S. R. Strong Exciton-Photon Coupling in an Organic Single Crystal Microcavity. *Phys. Rev. Lett.* **2008**, *101*, 116401.

(7) Schwartz, T.; Hutchison, J. A.; Genet, C.; Ebbesen, T. W. Reversible Switching of Ultrastrong Light-Molecule Coupling. *Phys. Rev. Lett.* **2011**, *106*, 196405.

(8) Kéna-Cohen, S.; Maier, S. A.; Bradley, D. D. C. Ultrastrongly Coupled Exciton-Polaritons in Metal-Clad Organic Semiconductor Microcavities. *Adv. Opt. Mater.* **2013**, *1*, 827.

(9) Bellessa, J.; Bonnand, C.; Plenet, J. C.; Mugnier, J. Strong Coupling between Surface Plasmons and Excitons in an Organic Semiconductor. *Phys. Rev. Lett.* **2004**, *93*, 036404.

(10) Dintinger, J.; Klein, S.; Bustos, F.; Barnes, W. L.; Ebbesen, T. W. Strong coupling between surface plasmon-polaritons and organic molecules in subwavelength hole arrays. *Phys. Rev. B* **2005**, *71*, 035424.

(11) Hakala, T. K.; Toppari, J. J.; Kuzyk, A.; Pettersson, M.; Tikkanen, H.; Kunttu, H.; Törmä, P. Vacuum Rabi Splitting and Strong-Coupling Dynamics for Surface-Plasmon Polaritons and Rhodamine 6G Molecules. *Phys. Rev. Lett.* **2009**, *103*, 053602.

(12) Vasa, P.; Pomraenke, R.; Cirmi, G.; De Re, E.; Wang, W.; Schwieger, S.; Leipold, D.; Runge, E.; Cerullo, G.; Lienau, C. Ultrafast Manipulation of Strong Coupling in Metal-Molecular Aggregate Hybrid Nanostructures. *ACS Nano* **2010**, *4*, 7559.

(13) Rodriguez, S. R. K.; Feist, J.; Verschuuren, M. A.; García Vidal, F. J.; Gómez Ri-

vas, J. Thermalization and Cooling of Plasmon-Exciton Polaritons: Towards Quantum Condensation. *Phys. Rev. Lett.* **2013**, *111*, 166802.

(14) Väkeväinen, A. I.; Moerland, R. J.; Rekola, H. T.; Eskelinen, A.-P.; Martikainen, J.-P.; Kim, D.-H.; Törmä, P. Plasmonic Surface Lattice Resonances at the Strong Coupling Regime. *Nano Lett.* **2014**, *14*, 1721.

(15) Baudrion, A. L.; Perron, A.; Veltri, A.; Bouhelier, A.; Adam, P. M.; Bachelot, R. Reversible strong coupling in silver nanoparticle arrays using photochromic molecules. *Nano Lett.* **2013**, *13*, 282.

(16) Zengin, G.; Wersäll, M.; Nilsson, S.; Antosiewicz, T. J.; Käll, M.; Shegai, T. Realizing Strong Light-Matter Interactions between Single-Nanoparticle Plasmons and Molecular Excitons at Ambient Conditions. *Phys. Rev. Lett.* **2015**, *114*, 157401.

(17) Graf, A.; Tropf, L.; Zakharko, Y.; Zaumseil, J.; Gather, M. C. Near-infrared exciton-polaritons in strongly coupled single-walled carbon nanotube microcavities. *Nat. Commun.* **2016**, *7*, 13078.

(18) Zakharko, Y.; Graf, A.; Zaumseil, J. Plasmonic Crystals for Strong Light–Matter Coupling in Carbon Nanotubes. *Nano Lett.* **2016**, *16*, 6504.

(19) Santhosh, K.; Bitton, O.; Chuntonov, L.; Haran, G. Vacuum Rabi splitting in a plasmonic cavity at the single quantum emitter limit. *Nat. Commun.* **2016**, *7*, 11823.

(20) Chikkaraddy, R.; de Nijs, B.; Benz, F.; Barrow, S. J.; Scherman, O. A.; Rosta, E.; Demetriadou, A.; Fox, P.; Hess, O.; Baumberg, J. J. Single-molecule strong coupling at room temperature in plasmonic nanocavities. *Nature* **2016**, *535*, 127.

(21) Liu, R.; Zhou, Z.-K.; Yu, Y.-C.; Zhang, T.; Wang, H.; Liu, G.; Wei, Y.; Chen, H.; Wang, X.-H. Strong Light-Matter Interactions in Single Open Plasmonic Nanocavities at the Quantum Optics Limit. *Phys. Rev. Lett.* **2017**, *118*, 237401.

(22) Sanvitto, D.; Kéna-Cohen, S. The road towards polaritonic devices. *Nat. Mater.* **2016**, *15*, 1061.

(23) Kéna-Cohen, S.; Forrest, S. R. Room-temperature polariton lasing in an organic single-crystal microcavity. *Nat. Phot.* **2010**, *4*, 371.

(24) Plumhof, J. D.; Stöferle, T.; Mai, L.; Scherf, U.; Mahrt, R. F. Room-temperature Bose–Einstein condensation of cavity exciton–polaritons in a polymer. *Nat. Mater.* **2013**, *13*, 247.

(25) Ramezani, M.; Halpin, A.; Fernández-Domínguez, A. I.; Feist, J.; Rodriguez, S. R.-K.; Garcia-Vidal, F. J.; Gómez Rivas, J. Plasmon-exciton-polariton lasing. *Optica* **2017**, *4*, 31.

(26) Daskalakis, K. S.; Maier, S. A.; Murray, R.; Kéna-Cohen, S. Nonlinear interactions in an organic polariton condensate. *Nat. Mater.* **2014**, *13*, 271.

(27) Feist, J.; Garcia-Vidal, F. J. Extraordinary Exciton Conductance Induced by Strong Coupling. *Phys. Rev. Lett.* **2015**, *114*, 196402.

(28) Gonzalez-Ballestero, C.; Feist, J.; Moreno, E.; Garcia-Vidal, F. J. Harvesting excitons through plasmonic strong coupling. *Phys. Rev. B* **2015**, *92*, 121402(R).

(29) Gonzalez-Ballestero, C.; Moreno, E.; Garcia-Vidal, F. J.; Gonzalez-Tudela, A. Non-reciprocal few-photon routing schemes based on chiral waveguide-emitter couplings. *Phys. Rev. A* **2016**, *94*, 063817.

(30) Lerario, G.; Ballarini, D.; Fieramosca, A.; Cannavale, A.; Genco, A.; Mangione, F.; Gambino, S.; Dominici, L.; De Giorgi, M.; Gigli, G.; Sanvitto, D. High-speed flow of interacting organic polaritons. *Light Sci. Appl.* **2017**, *6*, e16212.

(31) Barachati, F.; De Liberato, S.; Kéna-Cohen, S. Generation of Rabi-frequency radiation using exciton-polaritons. *Phys. Rev. A* **2015**, *92*, 033828.

(32) Barachati, F.; Simon, J.; Getmanenko, Y. A.; Barlow, S.; Marder, S. R.; Kéna-Cohen, S. Tunable third-harmonic generation from polaritons in the ultrastrong coupling regime. *arXiv:1703.08536*

(33) Michetti, P.; Mazza, L.; La Rocca, G. C. In *Organic Nanophotonics*; Zhao, Y. S., Ed.; Nano-Optics and Nanophotonics; Springer: Berlin, Heidelberg, 2015; p 39.

(34) González-Tudela, A.; Huidobro, P. A.; Martín-Moreno, L.; Tejedor, C.; García-Vidal, F. J. Theory of Strong Coupling between Quantum Emitters and Propagating Surface Plasmons. *Phys. Rev. Lett.* **2013**, *110*, 126801.

(35) Litinskaya, M.; Reineker, P.; Agranovich, V. M. Fast polariton relaxation in strongly coupled organic microcavities. *J. Lumin.* **2004**, *110*, 364.

(36) Mazza, L.; Kéna-Cohen, S.; Michetti, P.; La Rocca, G. C. Microscopic theory of polariton lasing via vibronically assisted scattering. *Phys. Rev. B* **2013**, *88*, 075321.

(37) Ćwik, J. A.; Reja, S.; Littlewood, P. B.; Keeling, J. Polariton condensation with saturable molecules dressed by vibrational modes. *EPL* **2014**, *105*, 47009.

(38) Canaguier-Durand, A.; Genet, C.; Lambrecht, A.; Ebbesen, T. W.; Reynaud, S. Non-Markovian polariton dynamics in organic strong coupling. *Eur. Phys. J. D* **2015**, *69*, 24.

(39) Spano, F. C. Optical microcavities enhance the exciton coherence length and eliminate vibronic coupling in J-aggregates. *J. Chem. Phys.* **2015**, *142*, 184707.

(40) Hutchison, J. A.; Schwartz, T.; Genet, C.; Devaux, E.; Ebbesen, T. W. Modifying Chemical Landscapes by Coupling to Vacuum Fields. *Angew. Chemie* **2012**, *124*, 1624.

(41) Wang, S.; Mika, A.; Hutchison, J. A.; Genet, C.; Jouaiti, A.; Hosseini, M. W.; Ebbesen, T. W. Phase transition of a perovskite strongly coupled to the vacuum field. *Nanoscale* **2014**, *6*, 7243.

(42) Zeng, P.; Cadusch, J.; Chakraborty, D.; Smith, T. A.; Roberts, A.; Sader, J. E.; Davis, T. J.; Gómez, D. E. Photoinduced Electron Transfer in the Strong Coupling Regime: Waveguide–Plasmon Polaritons. *Nano Lett.* **2016**, *16*, 2651.

(43) Ebbesen, T. W. Hybrid Light–Matter States in a Molecular and Material Science Perspective. *Acc. Chem. Res.* **2016**, *49*, 2403.

(44) Baieva, S.; Hakamaa, O.; Groenhof, G.; Heikkilä, T. T.; Toppari, J. J. Dynamics of Strongly Coupled Modes between Surface Plasmon Polaritons and Photoactive Molecules: The Effect of the Stokes Shift. *ACS Photonics* **2017**, *4*, 28.

(45) Galego, J.; Garcia-Vidal, F. J.; Feist, J. Cavity-Induced Modifications of Molecular Structure in the Strong-Coupling Regime. *Phys. Rev. X* **2015**, *5*, 041022.

(46) Flick, J.; Ruggenthaler, M.; Appel, H.; Rubio, A. Kohn–Sham approach to quantum electrodynamical density-functional theory: Exact time-dependent effective potentials in real space. *Proc. Natl. Acad. Sci.* **2015**, *112*, 15285.

(47) Ćwik, J. A.; Kirton, P.; De Liberato, S.; Keeling, J. Excitonic spectral features in strongly coupled organic polaritons. *Phys. Rev. A* **2016**, *93*, 033840.

(48) Herrera, F.; Spano, F. C. Cavity-Controlled Chemistry in Molecular Ensembles. *Phys. Rev. Lett.* **2016**, *116*, 238301.

(49) Kowalewski, M.; Bennett, K.; Mukamel, S. Non-adiabatic dynamics of molecules in optical cavities. *J. Chem. Phys.* **2016**, *144*, 054309.

(50) Kowalewski, M.; Bennett, K.; Mukamel, S. Cavity Femtochemistry: Manipulating Nonadiabatic Dynamics at Avoided Crossings. *J. Phys. Chem. Lett.* **2016**, *7*, 2050.

(51) Bennett, K.; Kowalewski, M.; Mukamel, S. Novel photochemistry of molecular polaritons in optical cavities. *Faraday Discuss.* **2016**, *194*, 259.

(52) Zeb, M. A.; Kirton, P. G.; Keeling, J. Exact spectral properties of vibrationally dressed polaritons. *arXiv:1608.08929*

(53) Flick, J.; Ruggenthaler, M.; Appel, H.; Rubio, A. Atoms and molecules in cavities, from weak to strong coupling in quantum-electrodynamics (QED) chemistry. *Proc. Natl. Acad. Sci.* **2017**, *114*, 3026.

(54) Flick, J.; Appel, H.; Ruggenthaler, M.; Rubio, A. Cavity Born–Oppenheimer Approximation for Correlated Electron–Nuclear-Photon Systems. *J. Chem. Theory Comput.* **2017**, *13*, 1616.

(55) Kowalewski, M.; Mukamel, S. Manipulating molecules with quantum light. *Proc. Natl. Acad. Sci.* **2017**, *114*, 3278.

(56) Martínez-Martínez, L. A.; Ribeiro, R. F.; Campos-González-Angulo, J.; Yuen-Zhou, J. Can ultrastrong coupling change ground-state chemical reactions? *arXiv:1705.10655*

(57) Galego, J.; Garcia-Vidal, F. J.; Feist, J. Suppressing photochemical reactions with quantized light fields. *Nat. Commun.* **2016**, *7*, 13841.

(58) Galego, J.; Garcia-Vidal, F. J.; Feist, J. Many-molecule reaction triggered by a single photon in polaritonic chemistry. *arXiv:1704.07261*

(59) Domcke, W., Yarkony, D. R., Köppel, H., Eds. *Conical Intersections: Electronic Structure, Dynamics and Spectroscopy*; Advanced Series in Physical Chemistry; World Scientific Publishing Co. Pte. Ltd., 2004; Vol. 15.

(60) Worth, G. A.; Cederbaum, L. S. Beyond Born-Oppenheimer: Molecular Dynamics Through a Conical Intersection. *Annu. Rev. Phys. Chem.* **2004**, *55*, 127.

(61) Levine, B. G.; Martínez, T. J. Isomerization Through Conical Intersections. *Annu. Rev. Phys. Chem.* **2007**, *58*, 613.

(62) Tully, J. C. Perspective: Nonadiabatic dynamics theory. *J. Chem. Phys.* **2012**, *137*, 22A301.

(63) Domcke, W.; Yarkony, D. R. Role of Conical Intersections in Molecular Spectroscopy and Photoinduced Chemical Dynamics. *Annu. Rev. Phys. Chem.* **2012**, *63*, 325.

(64) Dicke, R. Coherence in Spontaneous Radiation Processes. *Phys. Rev.* **1954**, *93*, 99.

(65) Tavis, M.; Cummings, F. W. Exact solution for an N-molecule-radiation-field Hamiltonian. *Phys. Rev.* **1968**, *170*, 379.

(66) Wu, N.; Feist, J.; Garcia-Vidal, F. J. When polarons meet polaritons: Exciton-vibration interactions in organic molecules strongly coupled to confined light fields. *Phys. Rev. B* **2016**, *94*, 195409.

(67) Herrera, F.; Spano, F. C. Dark Vibronic Polaritons and the Spectroscopy of Organic Microcavities. *Phys. Rev. Lett.* **2017**, *118*, 223601.

(68) Tokatly, I. V. Time-Dependent Density Functional Theory for Many-Electron Systems Interacting with Cavity Photons. *Phys. Rev. Lett.* **2013**, *110*, 233001.

(69) Ruggenthaler, M.; Flick, J.; Pellegrini, C.; Appel, H.; Tokatly, I. V.; Rubio, A. Quantum-electrodynamical density-functional theory: Bridging quantum optics and electronic-structure theory. *Phys. Rev. A* **2014**, *90*, 012508.

(70) Sisto, A.; Glowacki, D. R.; Martinez, T. J. Ab Initio Nonadiabatic Dynamics of Multichromophore Complexes: A Scalable Graphical-Processing-Unit-Accelerated Exciton Framework. *Acc. Chem. Res.* **2014**, *47*, 2857.

(71) Sisto, A.; Stross, C.; van der Kamp, M. W.; O'Connor, M.; McIntosh-Smith, S.; Johnson, G. T.; Hohenstein, E. G.; Manby, F. R.; Glowacki, D. R.; Martinez, T. J. Atomistic non-adiabatic dynamics of the LH2 complex with a GPU-accelerated ab initio exciton model. *Phys. Chem. Chem. Phys.* **2017**, *19*, 14924.

(72) Luk, H. L.; Feist, J.; Toppari, J. J.; Groenhof, G. Multiscale Molecular Dynamics Simulations of Polaritonic Chemistry. *J. Chem. Theory Comput.* **2017**, 10.1021/acs.jctc.7b00388.

(73) Shalabney, A.; George, J.; Hutchison, J.; Pupillo, G.; Genet, C.; Ebbesen, T. W. Coherent coupling of molecular resonators with a microcavity mode. *Nat. Commun.* **2015**, *6*, 5981.

(74) Simpkins, B. S.; Fears, K. P.; Dressick, W. J.; Spann, B. T.; Dunkelberger, A. D.; Owrutsky, J. C. Spanning Strong to Weak Normal Mode Coupling between Vibrational and Fabry–Pérot Cavity Modes through Tuning of Vibrational Absorption Strength. *ACS Photonics* **2015**, *2*, 1460.

(75) del Pino, J.; Feist, J.; Garcia-Vidal, F. J. Quantum theory of collective strong coupling of molecular vibrations with a microcavity mode. *New J. Phys.* **2015**, *17*, 053040.

(76) Bucksbaum, P. H.; Zavriyev, A.; Muller, H. G.; Schumacher, D. W. Softening of the H_2^+ molecular bond in intense laser fields. *Phys. Rev. Lett.* **1990**, *64*, 1883.

(77) Frasinski, L. J.; Posthumus, J. H.; Plumridge, J.; Codling, K.; Taday, P. F.; Langley, A. J. Manipulation of Bond Hardening in H_2^+ by Chirping of Intense Femtosecond Laser Pulses. *Phys. Rev. Lett.* **1999**, *83*, 3625.

(78) Sussman, B. J.; Townsend, D.; Ivanov, M. Y.; Stolow, A. Dynamic Stark Control of Photochemical Processes. *Science* **2006**, *314*, 278.

(79) Moiseyev, N.; Šindelka, M.; Cederbaum, L. S. Laser-induced conical intersections in molecular optical lattices. *J. Phys. B* **2008**, *41*, 221001.

(80) Demekhin, P. V.; Cederbaum, L. S. Light-induced conical intersections in polyatomic molecules: General theory, strategies of exploitation, and application. *J. Chem. Phys.* **2013**, *139*, 154314.

(81) Corrales, M. E.; González-Vázquez, J.; Balerdi, G.; Solá, I. R.; de Nalda, R.; Bañares, L. Control of ultrafast molecular photodissociation by laser-field-induced potentials. *Nat. Chem.* **2014**, *6*, 785.

(82) Schwartz, T.; Hutchison, J. A.; Léonard, J.; Genet, C.; Haacke, S.; Ebbesen, T. W. Polariton Dynamics under Strong Light-Molecule Coupling. *ChemPhysChem* **2013**, *14*, 125.

(83) Velha, P.; Picard, E.; Charvolin, T.; Hadji, E.; Rodier, J.; Lalanne, P.; Peyrade, D. Ultra-High Q/V Fabry-Perot microcavity on SOI substrate. *Opt. Express* **2007**, *15*, 16090.

(84) Akahane, Y.; Asano, T.; Song, B.-S.; Noda, S. High-Q photonic nanocavity in a two-dimensional photonic crystal. *Nature* **2003**, *425*, 944.

(85) Spillane, S. M.; Kippenberg, T. J.; Vahala, K. J. Ultralow-threshold Raman laser using a spherical dielectric microcavity. *Nature* **2002**, *415*, 621.

(86) May, V.; Kühn, O. *Charge and Energy Transfer Dynamics in Molecular Systems*; Wiley-VCH Verlag GmbH & Co. KGaA: Weinheim, Germany, 2011.

(87) Kucharski, T. J.; Tian, Y.; Akbulatov, S.; Boulatov, R. Chemical solutions for the closed-cycle storage of solar energy. *Energy Environ. Sci.* **2011**, *4*, 4449.

(88) Cacciarini, M.; Skov, A. B.; Jevric, M.; Hansen, A. S.; Elm, J.; Kjaergaard, H. G.; Mikkelsen, K. V.; Brøndsted Nielsen, M. Towards Solar Energy Storage in the Photochromic Dihydroazulene-Vinylheptafulvene System. *Chem. Eur. J* **2015**, *21*, 7454.

(89) Gurke, J.; Quick, M.; Ernsting, N. P.; Hecht, S. Acid-catalysed thermal cycloreversion of a diarylethene: a potential way for triggered release of stored light energy? *Chem. Commun.* **2017**, *53*, 2150.

(90) Rohatgi-Mukherjee, K. K. *Fundamentals of photochemistry*; New Age International, 2013; p 370.

(91) Yoshizawa, T.; Wald, G. Pre-Lumirhodopsin and the Bleaching of Visual Pigments. *Nature* **1963**, *197*, 1279.

(92) Polli, D.; Altoè, P.; Weingart, O.; Spillane, K. M.; Manzoni, C.; Brida, D.; Tomasello, G.; Orlandi, G.; Kukura, P.; Mathies, R. A.; Garavelli, M.; Cerullo, G. Conical intersection dynamics of the primary photoisomerization event in vision. *Nature* **2010**, *467*, 440.

(93) Irie, M.; Fukaminato, T.; Matsuda, K.; Kobatake, S. Photochromism of Diarylethene Molecules and Crystals: Memories, Switches, and Actuators. *Chem. Rev.* **2014**, *114*, 12174.

(94) Guentner, M.; Schildhauer, M.; Thumser, S.; Mayer, P.; Stephenson, D.; Mayer, P. J.; Dube, H. Sunlight-powered kHz rotation of a hemithioindigo-based molecular motor. *Nat. Commun.* **2015**, *6*, 8406.

(95) Zietz, B.; Gabrielsson, E.; Johansson, V.; El-Zohry, A. M.; Sun, L.; Kloo, L. Photoisomerization of the cyanoacrylic acid acceptor group – a potential problem for organic dyes in solar cells. *Phys. Chem. Chem. Phys.* **2014**, *16*, 2251.

(96) Bonačić-Koutecký, V.; Bruckmann, P.; Hiberty, P.; Koutecký, J.; Leforestier, C.; Salem, L. Sudden Polarization in the Zwitterionic Z1 Excited States of Organic Intermediates. Photochemical Implications. *Angew. Chem. Int. Ed.* **1975**, *14*, 575.

(97) Garraway, B. M. The Dicke model in quantum optics: Dicke model revisited. *Philos. Trans. R. Soc. A Math. Phys. Eng. Sci.* **2011**, *369*, 1137.

(98) Kasha, M. Energy Transfer Mechanisms and the Molecular Exciton Model for Molecular Aggregates. *Radiat. Res.* **1963**, *20*, 55.

(99) Eyring, H. The Activated Complex in Chemical Reactions. *J. Chem. Phys.* **1935**, *3*, 107.

(100) Virgili, T.; Coles, D.; Adawi, A. M.; Clark, C.; Michetti, P.; Rajendran, S. K.; Brida, D.; Polli, D.; Cerullo, G.; Lidzey, D. G. Ultrafast polariton relaxation dynamics in an organic semiconductor microcavity. *Phys. Rev. B* **2011**, *83*, 2.

(101) Gubbin, C. R.; De Liberato, S. Theory of Nonlinear Polaritonics: $\chi^{(2)}$ Scattering on a β-SiC Surface. *ACS Photonics* **2017**, *4*, 1381.

(102) Holstein, T.; Primakoff, H. Field Dependence of the Intrinsic Domain Magnetization of a Ferromagnet. *Phys. Rev.* **1940**, *58*, 1098.

(103) Sáez-Blázquez, R.; Feist, J.; Fernández-Domínguez, A. I.; García-Vidal, F. J. Enhancing Photon Correlations through Plasmonic Strong Coupling. *arXiv:1701.08964*

Graphical TOC Entry